Supplementary Material

The relationship between target strength frequency response and vertical swim velocity: a new approach for fish discrimination

Hikaru Homma* and Ilia Ostrovsky

Israel Oceanographic and Limnological Research, Yigal Allon Kinneret Limnological Laboratory, P.O. Box 447, Migdal 14950, Israel.

* Corresponding author.

E-mail address: hommalight@gmail.com

Affiliation: Israel Oceanographic and Limnological Research, Yigal Allon Kinneret Limnological Laboratory.

Address: P.O. Box 447, Migdal 14950, Israel.

Telephone: +972-4-6721444

Fax: +972-4-6724627

SM1. Single target and fish track detection

We used the software Echoview 9 (Echoview Software Pty. Ltd.) to obtain the echoes of single targets and tracks of the studied fish from the data of pulse-compressed wideband backscattering strength. The single target detection function of Echoview located the peaks of wideband backscattering strength vertical profile at each time step with the criteria for excluding overlapping targets, which is based on the conventional method for narrowband data (Ona and Barange, 1999). The detected peaks at each time step were defined as echoes from single targets. Using the detected single targets, the fish tracks were estimated by using the fish track detection function of Echoview (Blackman, 1986; Bertsekas, 1990). The single targets that were sequentially detected without noticeable jumps in depth, time, and the position in a beam were defined as a track of the same object (fish).

The fish track detection function was run with the parameters summarized in Table S1. We selected the “4D” algorithm (using range, major/minor-axis angles, and time) of the fish track detection function. More details about the algorithms and parameters of the function are described on the website of Echoview (Echoview Software Pty. Ltd., 2020).

In addition to the parameters shown in Table 1, the parameters of the acceptance of detected tracks were as follows:

Minimum number of single targets in a track = 3,

Minimum number of pings in track (pings) = 3,

Maximum gap between single targets (pings) = 5.

The false detections of the tracks due to unwanted targets (e.g., cage wireframe in this study) were excluded manually.

Table S1. Parameter values used in the fish track detection function of Echoview.

Parameters	Major axis	Minor axis	Range	TS	Ping gap
Alpha	0.7	0.7	0.7	-	-
Beta	0.5	0.5	0.5	-	-
Exclusion distance (m)	4.0	4.0	0.2	-	-
Missed ping expansion (%)	0.0	0.0	0.0	-	-
Weight	30	30	40	10	0

SM2. Calculation of frequency response

The frequency response of target strength depending on acoustic frequencies, TS(f), was calculated by using the Echoview based on the method suggested by Demer et al. (2017). The signal received by the echosounder was pulse compressed to improve time-domain resolution and signal-to-noise ratio (e.g., Chu and Stanton, 1998). First, the Echoview defined a short segment of the time series of the received signal which corresponds to a section of a vertical profile of backscattering strength around a single-target echo as the center of the section. Next, the short segment was transformed into frequency spectrum of the received signal by the fast Fourier transform (FFT) and the normalization using the frequency spectrum of transmitted signal. The received signal was padded with zeros, and the number of data points for FFT calculation was increased to 1024 to improve the frequency resolution of the resulting spectrum. The frequency spectrum of the received signal was converted into TS(f) by using the impedances of the receiver and transducer, the frequency dependent calibration coefficients, and compensations such as the range compensation of 40 log R (R is range), absorption, and beam compensation which are commonly used for the conversion from narrowband signal to target strength (e.g., Simmonds and MacLennan, 2005).

The frequency resolution of the resulting TS(f) is f_s/N, where f_s is the sampling rate of the received signal after decimations (Demer et al., 2017), N is the FFT length in data points. In this study, f_s was 62.5 kHz and N was 1024, thus the frequency resolution of TS(f) was ~0.06 kHz.

SM3. TS(f) quality control

The target strength frequency response, TS(f), was calculated from the wideband acoustic data covering the frequencies of 45 to 90 kHz. The curves of TS(f) showed an abrupt increase or decrease in TS near the boundaries of the frequency band (Fig. S1). To avoid such near-boundary sections, we confined the TS(f) curves by the lower and upper limits of 50 kHz and 85 kHz, respectively.

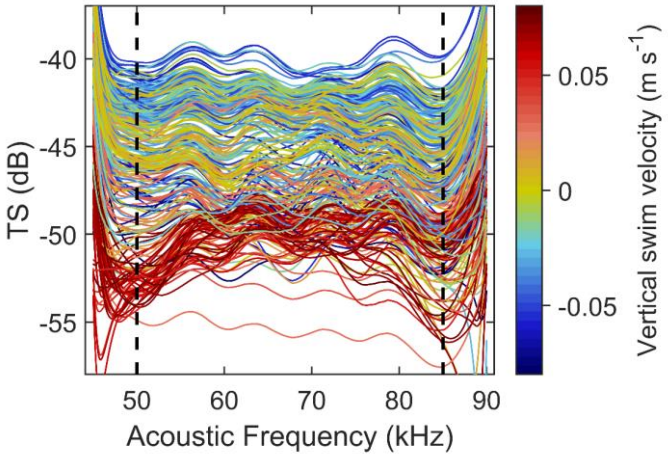

Fig. S1. Example of target strength frequency response, TS(*f*), at 45 to 90 kHz obtained from *Sarotherodon galilaeus* #1. Vertical dashed lines represent the upper and lower limits of the frequencies used for data analyses. Color bar indicates the vertical swim velocities of the fish for each TS(*f*).

Some TS(*f*) curves have extreme variations in TS with *f* and displayed irregular shapes (Fig. S2) comparatively to the majority of TS(*f*)s obtained from the same individual (Fig. S1). Such TS(*f*)s with atypical shapes could be attributed to interference of the fish signal with undefined objects, e.g. cage wireframe. Detection of most of the atypical TS(*f*) curves can be done, for example, by computation of TS standard deviation for each TS(*f*) curve. Then, we plotted the distribution of the TS standard deviation for each specimen and excluded the TS(*f*) outliers whose standard deviations exceeded their 90th percentile. The 90th percentile of the TS standard deviation varied between fish and

ranged 2.1 to 4.4 dB (Fig. S3). In addition, the atypical TS(*f*) curves with irregular shapes which were not detected by the TS standard deviation were removed manually.

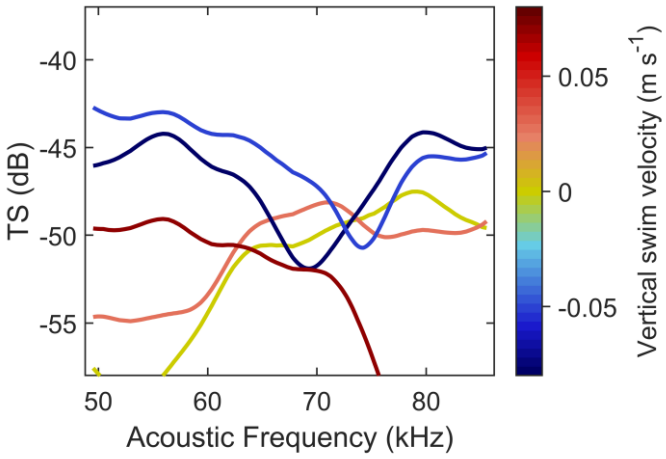

Fig. S2. Examples of the atypical target strength frequency responses, TS(*f*)s, of *Sarotherodon galilaeus* #1 with the irregular shapes, i.e., large variations of TS with *f* that were excluded from the data analyses. Color bar indicates the fish vertical swim velocity for each TS(*f*).

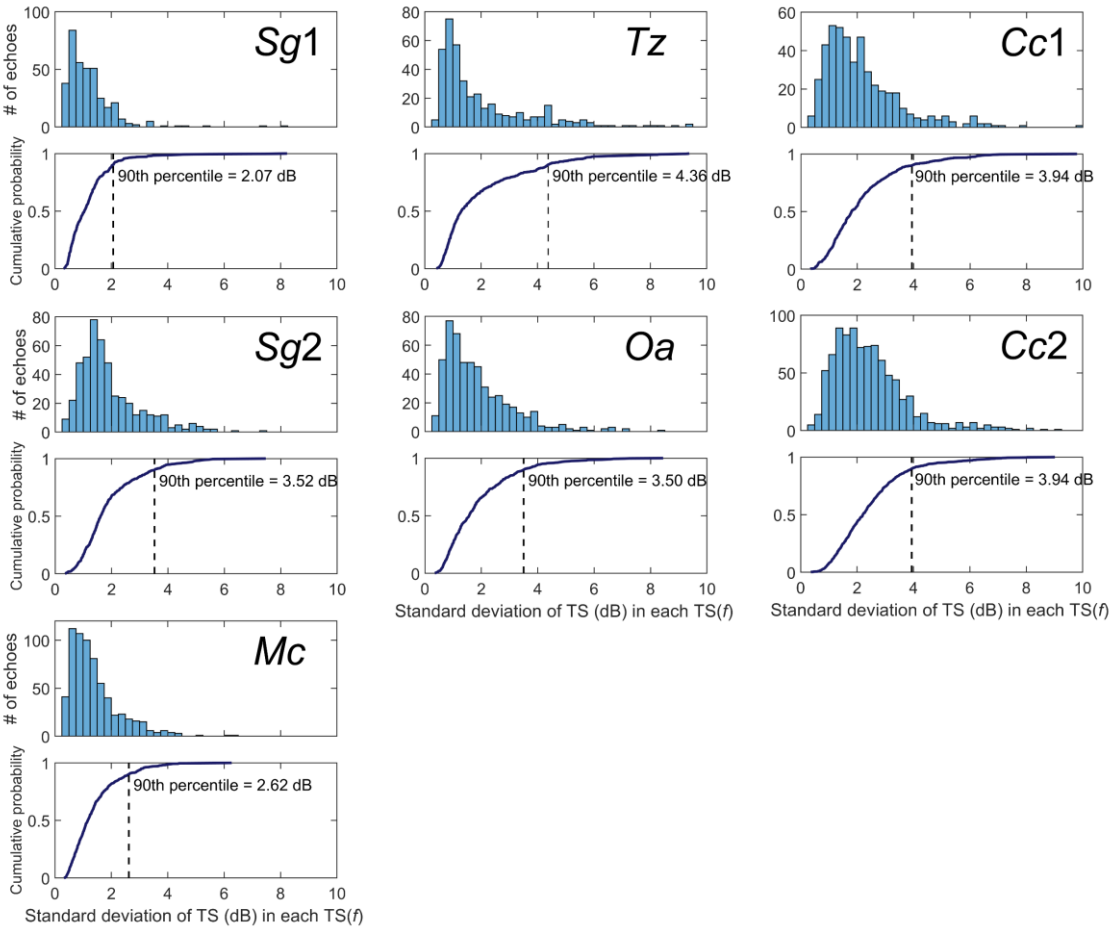

Fig. S3. Histograms of TS standard deviation calculated for each TS(*f*) curve and their empirical cumulative distribution function (see Table 1 in the main text for species abbreviations). For each studied fish, the 90th percentile was used as the threshold to exclude the TS(*f*)s with exceptionally large TS variations.

In addition, all single-target echoes positioned in close proximity (< 5 cm) to the top and bottom of the cage, where fish changed their swimming direction (flipped), were also excluded from the analyses, as they could impair the consistency between fish

vertical swim velocity (VSV) and fish body orientation in the cage with confined dimensions. For the same reason, for our analyses we used only the single-target echoes with a small variance of the VSV over 5 seconds centered at each time step. This permitted us to select the echoes when the fish was swimming at stable velocities. The upper threshold of the variance of the VSV over 5 seconds was set to 1.3×10^{-3} m^2 s^{-2}, which corresponds to the 95th percentile of the 5-second VSV variance measured from all studied specimens (Fig. S4).

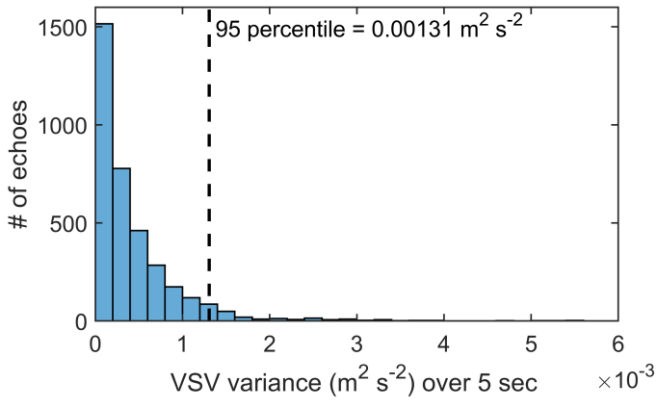

Fig. S4. Histogram of VSV variance over 5 sec measured from all studied fish. The 95th percentile of the VSV variance (vertical dashed line) was used as the threshold to remove the data with exceptionally large VSV variance.

SM4 Frequency responses of various fishes

Large variability of TS at given *f* (e.g. at 70 kHz) and TS(*f*) shapes were observed for all studied fishes (Fig. S5). The variations of TS(*f*) were associated mainly with VSV of fish. The variations of TS(70) were always >10 dB but in some cases (e.g. *Mc* and *Tz*) exceeded 20 dB.

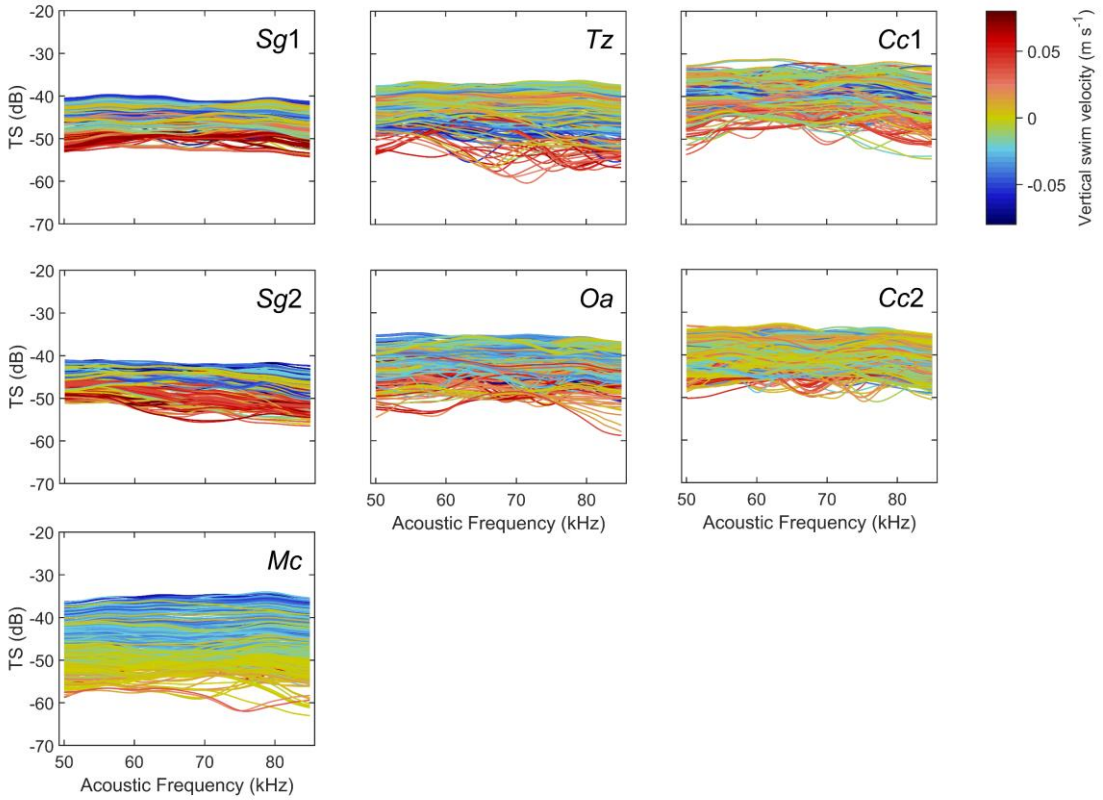

Fig. S5. Target strength frequency response, TS(*f*), from various fishes (see Table 1 in the main text for species abbreviations). The data show large variations in TS at each *f*. Color bar indicates the fish vertical swim velocity for each TS(*f*).

SM5. TS and fish position in the cage and acoustic beam

To examine if TS of studied fishes could be dependent on their position in the cage and the acoustic beam, TS at 70 kHz was plotted against fish depth and major/minor axis angles in the acoustic beam (Fig. S6). The relationships between the TS and the positions of different fishes did not reveal any patterns or trends. This indicates that the observed TS changes could not be associated with fish location in the cage and supports our conclusion that the TS changes were dependent on the VSV changes.

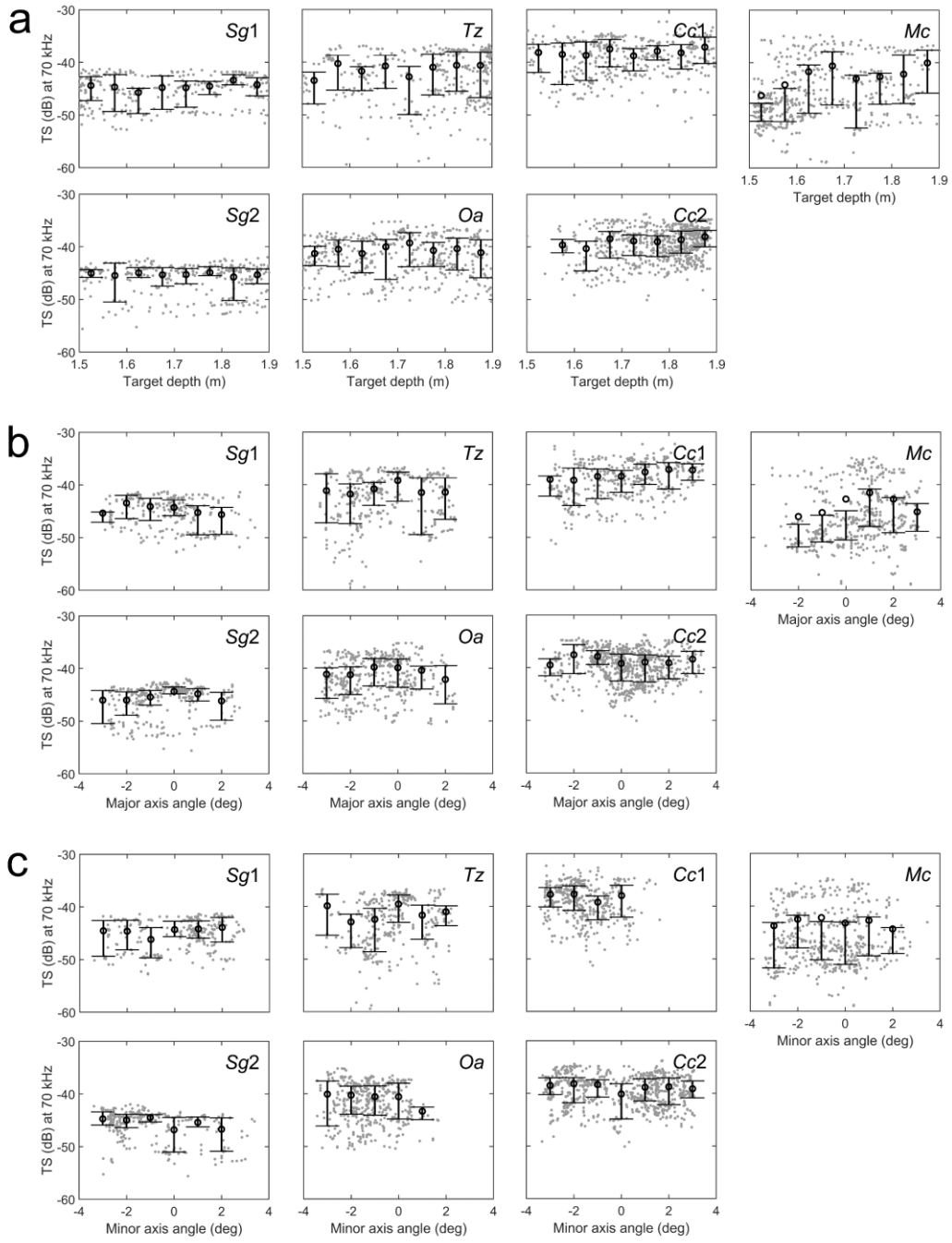

Fig. S6. Relationships between TS at 70 kHz and fish positions in the cage: (a) fish depth, (b) major axis angle of the fish in the acoustic beam, and (c) minor axis angle. See Table 1 in the main text for species abbreviations. Large empty dots and vertical bars represent the means and 25th–75th percentile ranges of TS at each (a) 0.05 m depth bin and (b,c)

1° angle bin. The relationships between the TS and fish positions did not show distinct patterns.

SM6. Relationships between vertical swim velocity and ΔTS at different frequencies

Figure S7 displays the relationships between the ΔTS(*f*, VSV) and vertical swim velocity, VSV, for *Sg*1. Different panels show the relationships at eight acoustic frequencies ranged from 50 to 85 kHz at 5-kHz intervals. This example demonstrates that the ΔTS-VSV relationships were similar for various frequencies. ΔTS increased with decreasing VSV and reached the maximum when VSVs were ranged between −0.05 m s^{-1} and −0.03 m s^{-1} at various frequencies.

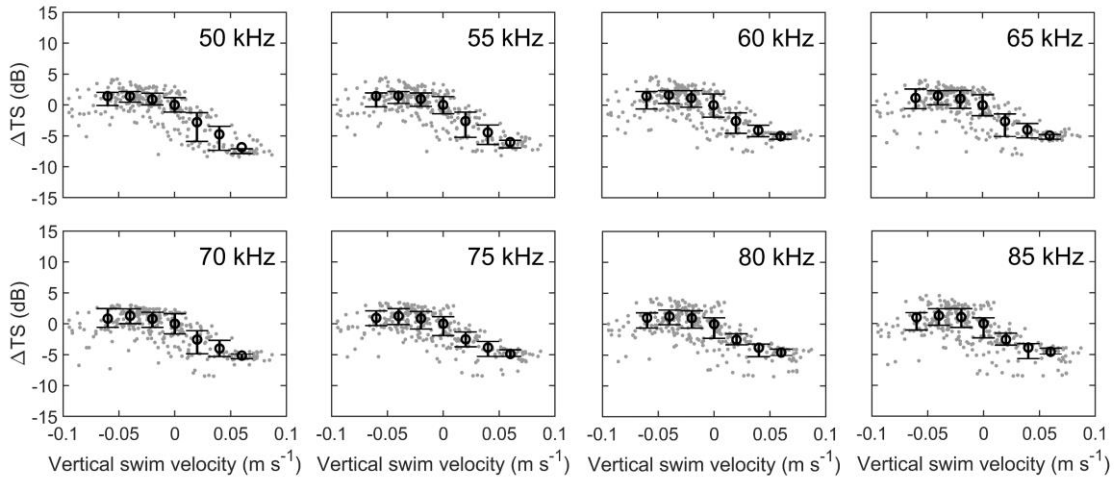

Fig. S7. Relationships between ΔTS (Eq. 1 in the main text) and vertical swim velocity at different acoustic frequencies for *Sg*1. Large empty dots and vertical bars represent the means and 25th–75th percentile ranges of ΔTS at each 0.02 m s^{-1} bin. The relationships show close similarities in patterns at various frequencies.

SM7. Near-field effect

The field close to a transducer or backscatterer is termed the near field, where the relationship between acoustic intensity and range is more complicated than that out of the near field (e.g., Simmonds and MacLennan, 2005). The near-field range of the transducer, R_{nf}, is calculated as follows (Demer et al., 2015):

$$R_{nf} = \frac{\pi {d_t}^2}{4\lambda}, \quad \text{(S1)}$$

where λ is the acoustic wavelength, and d_t is the largest distance across the active elements of a transducer. The d_t is approximated as follows (Demer et al., 2015):

$$d_t \cong \frac{3.2}{k \sin(\theta_{-3\ \mathrm{dB}}/2)}, \quad \text{(S2)}$$

where $\theta_{-3\ \mathrm{dB}}$ is the nominal half-power (3-dB) beamwidth, and $k = 2\pi/\lambda$ is the acoustic wavenumber. Demer et al. (2015) recommended measuring the backscattering strength at range > $3R_{nf}$ where the near-field effect can be negligible.

For the nominal frequency of 70-kHz transducer, R_{nf} is 1.2 m. Since the fish cage was situated 1.3–1.85 m from the transducer face (i.e., within the $3R_{nf}$), the acoustic data collected in the shallow pond could be potentially affected by the near-field effect. The investigations carried out by Rodríguez-Sánchez et al. (2016) did not reveal significant difference in the mean TS between the fish observed within the near field and the same individual observed well apart from the near field. These authors also concluded that the TS showed significant dependence on species and swimming orientation rather than the distance from the transducer. Despite we cannot exclude the impact of the near-field conditions on the absolute TS values, our results clearly show that the observed patterns of the ΔTS-VSV relationships were species characteristic. This suggests that the approach for species discrimination proposed in this study can be performed based on analysis of the ΔTS(f)-VSV relationships for different species. Still, further detailed investigations are needed to evaluate the proposed method under the better experimental conditions.

References

Bertsekas DP. 1990. The Auction Algorithm for Assignment and Other Network Flow Problems: A Tutorial. *Interfaces* 20(4): 133–149.

Blackman SS. 1986. Multiple-target tracking with radar applications, Dedham, Artech House.

Chu D, Stanton TK. 1998. Application of pulse compression techniques to broadband acoustic scattering by live individual zooplankton. *J. Acoust. Soc. Am.* 104(1): 39–55.

Demer DA, Berger L, Bernasconi M, Bethke E, Boswell K, Chu D, Domokos R, et al. 2015. Calibration of acoustic instruments, Copenhagen, ICES. ICES Cooperative Research Report No. 326.

Demer DA, Andersen LN, Bassett C, Berger L, Chu D, Condiotty J, Cutter GR, et al. 2017. 2016 USA–Norway EK80 Workshop Report: Evaluation of a wideband echosounder for fisheries and marine ecosystem science, Copenhagen, ICES. ICES Cooperative Research Report No. 336.

Echoview Software Pty. Ltd. 2020. Fish tracking algorithm. https://support.echoview.com/WebHelp/Reference/Algorithms/Fish_tracking_module/Fish_tracking_algorithms.htm (accessed 1 April 2021).

Ona E, Barange M. 1999. Single-target recognition. In: Ona E. (Ed.), Methodology for Target Strength Measurements, Copenhagen, ICES, pp. 28–43. ICES Cooperative Research Report No. 235.

Rodríguez-Sánchez V, Encina-Encina L, Rodríguez-Ruiz A, Sánchez-Carmona R. 2016. Do close range measurements affect the target strength (TS) of fish in horizontal beaming hydroacoustics? *Fish. Res.* 173(1): 4–10.

Simmonds EJ, MacLennan DN. 2005. Fisheries Acoustics: Theory and Practice. Second Edition, Oxford, Blackwell Publishing.